




Effect of metalation on some graphene nanoribbons for potential application as donor in organic photovoltaic cells

E. Mainimo¹, G. W. Ejuh^{2,3,*} , and J. M. B. Ndjaka¹

¹ Faculty of Science, Department of Physics, University of Yaoundé I, P.M.B 812, Yaoundé, Cameroon

² Department of Electrical and Electronic, Engineering, National Higher Polytechnic Institute, University of Bamenda, P. O. Box 39, Bamili, Cameroon

³ IUT-FV Bandjoun, Department of General and Scientific Studies, University of Dschang, P.M.B 134, Bandjoun, Cameroon

Received: 5 October 2020

Accepted: 15 October 2020

Published online:

4 November 2020

© Springer Science+Business Media, LLC, part of Springer Nature 2020

ABSTRACT

The present work is a systematic and theoretical study performed on three organometallic p-conjugated molecules based on graphene nanoribbons (GNRs) to act as potential donor material in organic photovoltaic cells, using the rhf, b3lyp and bpbe methods together with the 6–31 + g(d,p) basis. Analysis is made on HOMO, LUMO, bandgap, reorganization energy, open circuit voltage, the driving force, and nonlinear optical properties. These organic photovoltaic properties are predicted with the aid of PCBM as modelled acceptor. Results reveal positive agreement with traditional classical and experimental organic values, presenting the fact that metalated GNRs may be used as an effective and potential donor of electron in organic Bulk Heterojunction solar cells, owing to its enhanced nonlinear and photovoltaic properties. The values obtained for the reorganization energy, driving force and nonlinear optical properties are promissory properties that may be directly implemented in the investigated photovoltaic material. The power conversion efficiency obtained for Rb-perylene is seen to be around the maximum current value for organic photovoltaic cell. Rb-perylene shows the best organic photovoltaic properties followed by k-azulene then k-phenanthrene. The methodological approach offered in this research might aid in computer assisted-design of OPV materials.

1 Introduction

Global demand for energy is steadily increasing, consequently the total world energy demand use will surge at a typical annual rate of 1.8% to reach 18.49

TW in 2030 [1]. The usage of environmental friendly eco material, is of critical concern in the assembly of systems for renewable energy applications. Incidentally, the search for organic photovoltaic (OPV) molecules for solar cells technological

Address correspondence to E-mail: gehwilsonnejuh@yahoo.fr

implementation, has become a subject of passionate research in the last years. The task of acquiring new renewable energy sources to fill the energy gap is daring with photovoltaic solar energy being a promising research avenue to fill the energy deficit. Nevertheless, harnessing solar energy into electrical energy at low cost is no easy job. By 2019, the world record for solar cell efficiency developed by National Renewable Energy Laboratory, Golden, Colorado, USA stood at 47.1% realized with the use of multi-junction concentrator solar cells [2, 3]. Photovoltaic solar cells produced from inorganic matter, such as silicon have some limitation in terms of scarcity, toxicity, unconstrained resource storage, expensiveness and unmodifiable energy levels [4]. Faced with such limitation, attention is now directed to polymer or organic photovoltaic cells (OPVCs) due to the numerous virtues of organic material over their inorganic counterpart in mechanical flexibility, modifiable energy level, environmentally friendliness and low cost. Moreover, there exist immeasurable variety of organic molecules to choose from, for design purposes with very great tunable and optical absorption. However, OPVCs possess a disapproving low power conversion efficiency (PCE) than inorganic photovoltaic cells, ensuing from their large band gaps [5–19]. Besides having a low efficiency, OPVCs have low strength and stability and are more prone to water and oxygen attacks [20]. Accordingly, it remains a great challenge to achieve high performant OPVCs for practical purposes. Despite tremendous efforts put in the research of OPVCs they still lag far behind those of their inorganic counterparts in the power conversion efficiency (PCE).

The architecture of OPV cell is shown in Fig. 1 and habitually consists of an organic bilayer or a bulk heterojunction (BHJ) which is a sandwich of donor (D) and an acceptor (A) material between two different electrodes. The mechanism by which an OPVC, generates a photocurrent somehow differs from an inorganic PV semiconductor cell. While inorganic PV cell produce free carriers when they absorb photons, OPVCs generate excitons, which dissociates at the D–A interface due to a strong electrostatic field set up at the said interface. The electrostatic field arises from D and A, having different Electron Affinity (EA) whose value is usually chosen carefully to cause the exciton dissociation. The dissociated electron is conveyed to the acceptor material and then to the cathode, while the hole travels backwards through the donor

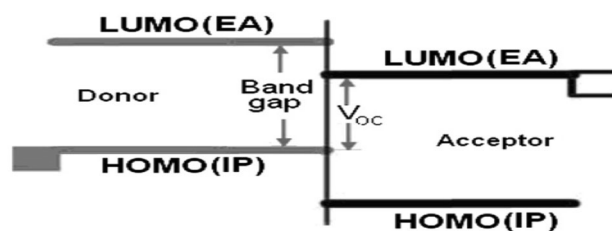


Fig. 1 Schematic energy diagram of a D–A interface bulk heterojunction solar cell

semiconductor to be collected at the anode. By 2012, research had realized a PCE for the best performing OPVC of not more than 10% [21–24].

A comprehension of the energy loss mechanisms and its limitation arising from the optical excitation process in the OPVC, to the collection of charge at the electrodes ought to lead to greater efficiencies in the near future with single heterojunction. However, higher efficiencies could emanate from stacking of multiple cells [25, 26]. The interrelatedness between photo electronic properties and molecular structure can't be overemphasized, so reasonable structural modifications can effectively improve the PCEs of the device. The optoelectronic and photovoltaic properties of an organic polymer could be tuned by chemical tailoring of the molecular structure. This has motivated the molecular modification of the organic polymers in this research paper; by metalating (adding metal) some selected graphene nanoribbons (GNRs) to foster device performance of its photovoltaic properties. Similar chemical engineering has been used to generate organic systems with electronic properties tailored to produce more performant PV cells [27]. GNRs have shown technologically relevance and potential applications, in areas such as gas electrode sensors, ultracapacitors, organic photovoltaic, optical information processors, integrated circuits and memories transistors [28–31]. Organic semiconductors of small structure are appropriate for large scale fabrication, have high dispersity, show good reproducibility and easy purification. A majority of small organic semiconductors utilized in solar cells, possess a push–pull architecture consisting of an electron donor and acceptor. This type of architecture is aimed at enhancing the intramolecular charge transfer (ICT) thereby narrowing the band gap and yielding higher solar absorptivity and more red-shifted ultraviolet–visible (UV–Vis) absorption spectra of the acceptors. Alteration of the donor group closes the band gap, a decisive factor in the

performance of photovoltaic cells [32]. Nonetheless difficulties in predicting precisely the properties of the novel molecular system, prior to its actual synthesis after modification deserves a theoretical calculation which could be vital in restricting effort of trial and-error synthesis.

This work is aimed at theoretically investigating the effect of adding metal (metalation) to some p-conjugated graphene nanoribbons-based molecules on their optical and electronic properties, using rhf, b3lyp and BPBE theory, in order to act as potential donor in BHJ OPVCs. The GNRs under investigation are phenanthrene, azulene and perylene. The novel structure; the metalated GNRs or the GNRs metal derivative is characterized and model as donor material against the most widely used acceptor, [6, 6]-phenyl-C61 butyric acid methyl ester (PCBM) [20, 33, 34] with the advantage that PCBM has a noble three-dimensional transport within its spherical structures; secondly, its charge mobility is extraordinary, thirdly there is swift and efficient charge transfer from the chosen donor material to its LUMO level. The metalated GNR is obtained by replacing hydrogen in the GNR by an alkali metal.

2 Computational detail

The donor compound; the metalated GNR in the ground state is investigated through the ab initio rhf and two Density Functional Theory (DFT) methods; the B3LYP and the BPBE method. The Becke3LYP (B3LYP) method incorporates a 3 constraint density functional named as Becke's gradient correction exchange [35], the Lee, Yang and Parr correlation functional [36] while the BPBE method, incorporates Beck's 1988 exchange functional (B) [35] with the 1996 functional of Perdew, Burke and Ernzerhof (PBE) [37, 38], with this method having the advantage that its incorporates a relatively large amount of non-local exact Hartree–Fock exchange (42%). These methods are employed along with the 6–31 + G(d, p) basis set. There is stability of the optimized geometries realized and align the minima on the energy surface, analyses made indicate nonexistence of imaginary frequencies. We employ Gaussian 09 quantum program in all computations [39]. Gauss View 5.0 is employed for realizing data and displaying the outcomes of the output [40]. DFT method has the feature of the inclusion of electron correlation, and is an invaluable

tool in molecular modelling of electronic properties, due to its laudable accuracy/computational-time. DFT calculations, are the standard approach for computations on metal containing systems, moreover, the DFT is very instrumental in designing molecules for NLO applications [41, 42] and for studying of electronic properties of solids [43–46]. The LUMO, HOMO and band energies are obtained directly from the optimized structured. The theoretical methodology is a compelling tool that overwhelms the difficulties in the experimental synthesis, explore alternatives, thereby lessening cost of material processing and production.

To maximize OPVC device performance, it is crucial to understand the parameters that determine its operational capability. These parameters include, band gap E_g , open circuit V_{oc} , driving force ΔE_{LL} , reorganization energy λ , the isotropic polarizability α , first-order hyperpolarizability β and anisotropy $\Delta\alpha$ of the organic material [20, 34]

The power conversion efficiency (PCE) is a key quantity used to characterize the cell performance of solar cell and depends on the band gap E_g , the open circuit voltage V_{oc} , current density J_{sc} , and fill factor FF . The PCE indicates the ratio of the electrical power produced by the solar cell per unit area measured in watts, divided by the watts of incident light under certain specified conditions called “standard test conditions [1]. The open circuit voltage will be calculated using the Scharber model [15, 47–49]

$$V_{oc} = \frac{1}{e} |E_H^D - E_L^A| - E_b \quad (1)$$

where e is the elementary charge, E_H^D is the HOMO energy of the donor, E_L^A is the LUMO energy of the acceptor and customary to agreed experimental laboratory value $E_L^A = -4.026$ eV for the acceptor PCBM [50], E_b the exciton binding energy for the electron and hole with a value ranging from 0.1 to 1 V, we take the value of 0.3 V as reported in other literature as the value is the loss factor associated to the heterojunction design [51–54].

The energy difference between the LUMO of the donor and acceptor ΔE_{LL} , called the driving force is an important factor that enhances the PCE of OPVCs, it is expressed as in [55]. The driving force is a determining factor for exciton dissociation to free charges at the D–A heterojunction.

$$\Delta E_{LL} = E_L^D - E_L^A \quad (2)$$

The free charges produced by exciton dissociation at the D–A heterojunction must travel through the active layer to reach the electrodes where they are collected to produce photocurrent. Charge carrier mobility estimated through the reorganization energy is therefore important in determining device efficiency. The electron and hole reorganization energies according to the Marcus model [56], are evaluated by the adiabatic potential-energy surface method. As we are characterizing a donor material which transport holes after exciton dissociation, we concern with hole reorganization energy λ_h calculated in literature [42, 57–61] as

$$\lambda_h = (E_0^+ - E_+^+) + (E_+^0 - E_0^0) \quad (3)$$

E_+^+ and E_0^0 represent energy of cation form and the neutral species in the optimized geometry, while E_+^0 and E_0^+ signify the energy of cation in neutral form and the energy of the neutral molecule in cationic geometry, respectively.

The nonlinear optical properties viz; the isotropic polarizability α , first-order hyperpolarizability β and anisotropy of the polarizability $\Delta\alpha$ are computed using the following equation [41, 62, 63], and give the extent of the delocalization of intramolecular charge of donor electrons in the OPVC.

$$\alpha = \frac{\alpha_{xx} + \alpha_{yy} + \alpha_{zz}}{3} \quad (4)$$

$$\Delta\alpha = \left[\frac{1}{2} \left((\alpha_{xx} - \alpha_{yy})^2 + (\alpha_{xx} - \alpha_{zz})^2 + (\alpha_{yy} - \alpha_{zz})^2 + 6(\alpha_{xy} + \alpha_{xz} + \alpha_{yz})^2 \right) \right]^{1/2} \quad (5)$$

$$\beta = \left((\beta_{xxx} + \beta_{xyy} + \beta_{zzz})^2 + (\beta_{yyy} + \beta_{yxx} + \beta_{yzz})^2 + (\beta_{zzz} + \beta_{zxx} + \beta_{zyy})^2 \right)^{1/2} \quad (6)$$

3 Results and discussion

3.1 Optimized geometric structure of the molecules

The optimized geometric structure obtained from calculations are shown in Fig. 2. As can be observed, the optimized structure of the metalated GNRs are planar.

3.2 Organic photovoltaic properties of the metalated GNRs

3.2.1 Open circuit voltage, driving force band gap, and density of state analysis

These calculated values determining photovoltaic performance of the metalated GNRs obtained from optimized geometry using the rhf, b3lyp and BPBE method are summarized in Table 1.

The open-circuit voltage V_{oc} , is the peak voltage across an OPV device. V_{oc} is obtained when the photogenerated current is balanced to zero, a state called flat band condition. The V_{oc} value is a useful parameter to indicate solar cell performance or power conversion efficiency of a solar cell device of type Bulk Heterojunction (BHJ). Enhancing V_{oc} is important in boosting the PCE of the solar cell.

The computed values of V_{oc} at the two dft methods are less than the 1 V required minimum value required for OPVC operation [64] but attain this target at the rhf method for all the three molecules. K-phenanthrene has the greatest value for V_{oc} at each level of theory than any of the rest two molecules except for Rb-perylene at the bpbe/6–31 + g(d,p) level of theory. Careful examination indicates that V_{oc} has a near inverse relationship trend with the hyperpolarizability as indicated in Fig. 3 suggesting increased intramolecular charge transfer may diminish V_{oc} . The computed V_{oc} values especially at the two dft levels are smaller than the practical values for OPVCs stated in literature for devices that have reasonable photocurrents [65]. However, hope to improve these values could dwell on other determining factors for V_{oc} , such as: donor energy levels, chemical potential gradients, light intensity, morphology (rough or smooth surface), external fluorescence, recombination of charge-carrier, light-source, cell temperatures, charge-carrier recombination, Fermi level pinning [66, 67].

A salient factor limiting the PCE of OPVCs is large energy loss, largely ascribed to the relatively large non-radiative recombination loss caused by the significant energy-level offset between the donor and acceptor as well as the extremely low electroluminescence quantum efficiency of organic photovoltaic materials. The energy-level offset between D–A interface cause exciton dissociation and is a vital step in OPVC functioning. This is measured through the driving force ΔE_{LL} and ought to be superior to

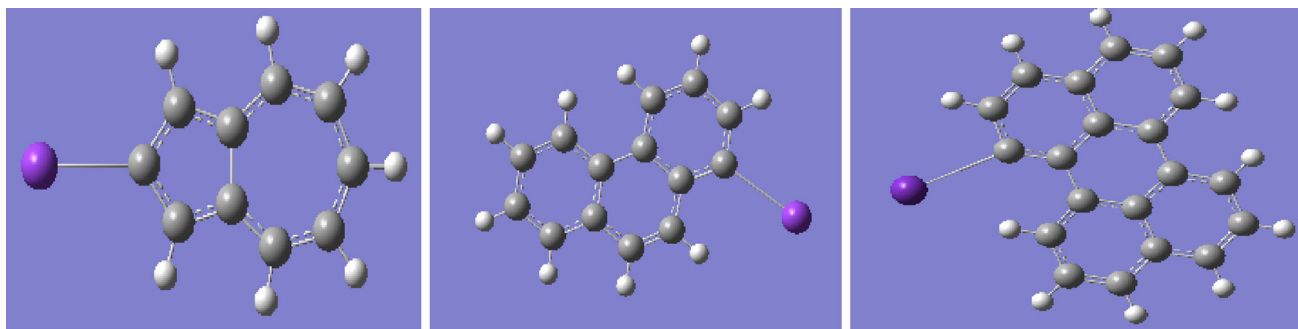
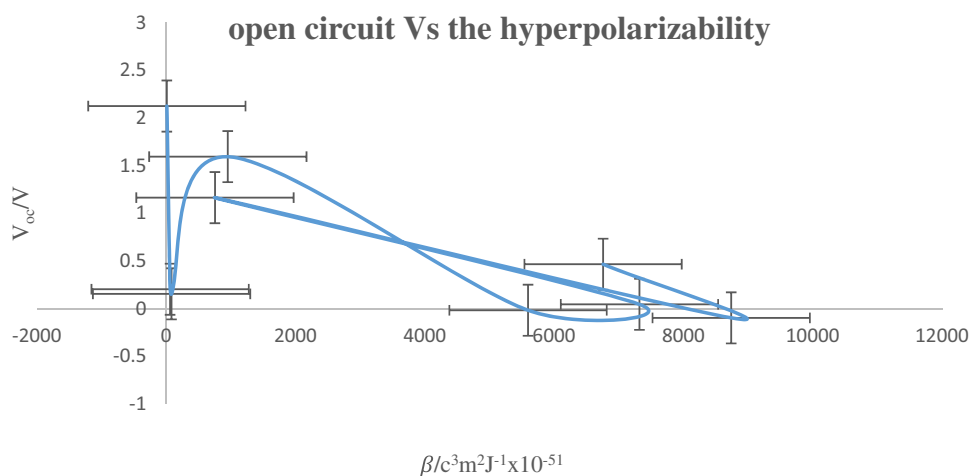


Fig. 2 Optimized structures of metalated azulene, phenanthrene and perylene respectively, using Rhf, B3lyp and Bpbe methods

Table 1 Organic photovoltaic and nonlinear properties of the metalated GNRs obtained using the BPBE method

Property	k-phenanthrene			k-azulene			Rb-perylene		
	Rhf	B3lyp	bpbe	Rhf	B3lyp	bpbe	Rhf	B3lyp	bpbe
E_L^D/eV	-0.42	-1.73	-1.69	-0.32	-1.61	-1.61	-0.48	-1.93	-2.15
E_H^D/eV	-6.45	-4.53	-3.57	-5.92	-4.31	-3.68	-5.49	-4.23	-3.26
E_{gap}^D/eV	6.02	2.80	1.87	5.60	2.71	1.99	5.01	2.30	1.10
E_L^A/eV	-4.026	-4.026	-4.026	-4.026	-4.026	-4.026	-4.026	-4.026	-4.026
V_{oc}/V	2.124	0.204	0.156	1.594	-0.016	0.046	1.164	-0.096	0.466
$\Delta E_{LL}/eV$	3.606	2.296	2.336	3.706	2.416	2.416	3.546	2.096	1.876

Fig. 3 Open circuit voltage against the hyperpolarizability for K-phenanthrene, K-azulene and Rb-perylene



0.30 eV in order to provide sufficient exciton dissociation [34, 55]. The driving force sets up electrostatic forces at the D–A interface, and when appropriately chosen the electric field generated, can split the excitons into holes and electrons efficiently. From Table 1, we remark that all the metalated GNRs have a ΔE_{LL} value that is above the 0.3 eV requirement, with k-azulene having the highest value of 3.706 eV. k-azulene equally shows the best results in exciton

dissociation than the other two GNRs metal derivatives at any level of theory. Inclusion of electron correlation effects are seen to diminish the driving force for exciton dissociation. After exciton dissociation the electrons are conveyed by the acceptor material with higher electron affinity than any of the 3 test donor materials and the hole by the donor material with lower ionization potential [20]. However, the efficiency of this process is greatly

hampered by recombination of charges and organic imperfections trapping.

One of the major impediments to get high PCE is the limited spectral overlap between the solar spectrum and its absorption by the photoactive donor material, consequently giving a small valued photocurrent. Actually, the total solar photon flux of approximately 62% is at wavelengths $\lambda > 600$ nm with almost 40% in the red and near-infrared (NIR) spectrum at $600 < \lambda < 1000$ nm. Nonetheless, the optical bandgap of most organic photoactive materials is not optimized with respect to the solar spectrum, in which only 20–30% of solar spectrum can be absorbed [1]. This indicate that we need to research new materials that will absorb NIR radiation, and efficiently transform the absorbed photons into electricity, such materials are those with bandgap below 1.9 eV [1, 20]. The band gap, a representative signature in photovoltaic materials, for the studied metalated GNRs stands at value of below 1.9 eV only at the bpbe/6–31 + g(d,p) level of theory for all three metal GNRs, with the least value obtained with Rb-perylene of 1.10 eV which could in theory guarantee the highest sunlight harvest efficiency as it has the greatest overlap with the sun spectrum. Rb-perylene also give the smallest band gap than any of the molecules at all level of theory. The rhf and the b3lyp method gives a band gap greater than the 1.9 eV required value for the operation of OPVCs. Non-inclusion of electron correlation effects in the rhf method widens the band gap. Small band gap OPVC materials optimize photon harvesting as they have great overlap with the sun spectrum. On comparing the band gap of these molecules with their inorganic counterparts, bearing in mind that functional inorganic photovoltaic devices operate within a band gap range of 0.7 eV to 2.5 eV [50], we observe they can be classified as small band gap material. The total density of state (DOS) spectrum for the studied molecules obtained using the RHF/6–31 + g(d,p), and bpbe/6–31 + G(d,p) level of theory in gas phase is presented in Fig. 4, showing the DOS spectrum with highest band gap and lowest band gap, respectively. The role of the various HOMO and LUMO groups of molecular orbitals are presented: in green for HOMO orbital and red for LUMO orbital. We perceive the very large energy gap for the rhf and small energy gap for bpbe methods. In BHJ type of OPVC, low-band gap organics serve myriad role of electron donors, hole transport, exciton generation, migration

and recombination. According to a criteria set to approximate the value of the PCE of an OPV by Scharber et al. in the literature [53], by matching the band gap and the LUMO level of the donor, accordingly a material having band gap smaller than 1.74 eV together with a $E_{LUMO} < -3.92$ eV, should generate a PCE of greater than 10%. Therefore, Rb-perylene at the bpbe/6–31 + g(d,p) level of theory, with a theoretical bandgap of 1.10 eV and $E_{LUMO} = -2.15$ eV could on such criteria enjoy a PCE of about 10%. Such efficiency realized in this research could in theory, get this organic polymer a step closer to commercialization. The band gap and the hyperpolarizability as shown in Fig. 5, show also a near inverse relationship, interestingly giving a similar shape to that portrayed by the V_{oc} and β . This inverse proportionality corroborates earlier results found in literature [68], due to significant extension of the conjugation of pi-electrons as a result of intramolecular charge transfer across the donor–acceptor bridge. The functioning of the OPVC has a stage by stage associated energy loss mechanism, such as non-absorbed photons, exciton decay as it diffuses to the D–A interface, geminate recombination of the bound electron hole pair as it disassociates into free carriers, and bimolecular recombination as the free carriers transport towards the electrodes for collection. The interrelatedness of these stages can't be underestimated. Improving a single stage could but not necessarily lead to the overall improvement of its functionality.

3.2.2 Reorganization energy and charge mobility

In designing novel solar cell devices there is need of linking charge transport properties and the molecular structure of the conjugated material. Reorganization energy of a molecular system cast a profound understanding of structure and charge transfer property relationship. The hole reorganization energy is key in determining charge carrier mobility in the donor and influences parametric hole coupling. High hole mobility for charge-carrier leads to high short circuit current, and is a central parameter for OPV materials as it impacts, extraction and recombination dynamics of charge. It's factual that low reorganization energy leads to a high charge mobility [69–71]. We observe from Table 2, with satisfaction that the reorganization energy of the metal substituted GNRs compounds are of a small value and are

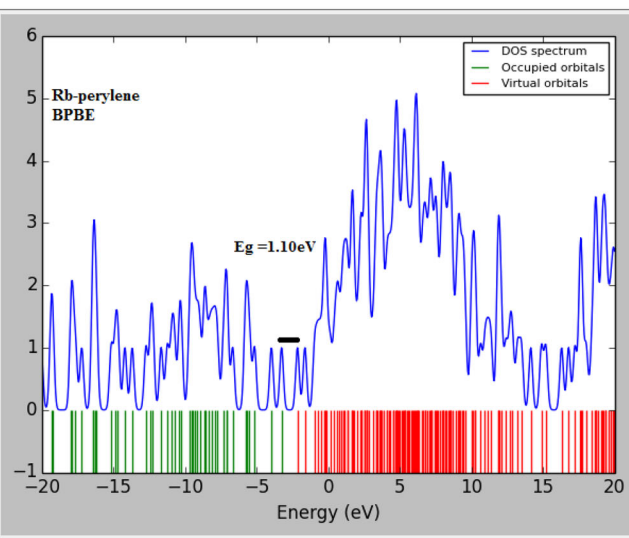
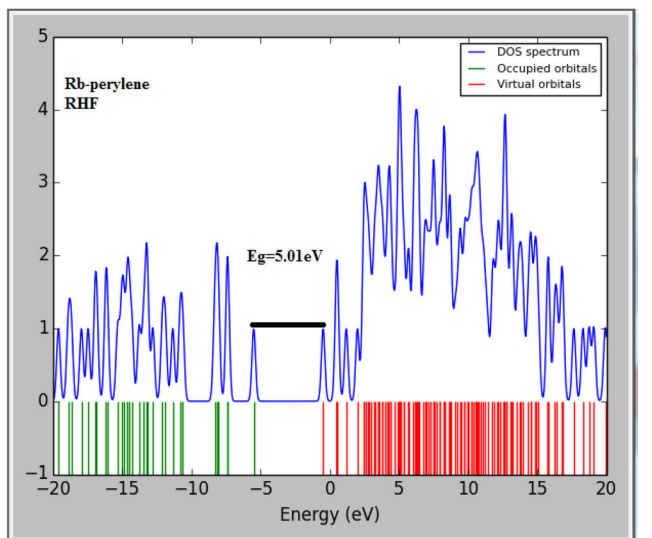
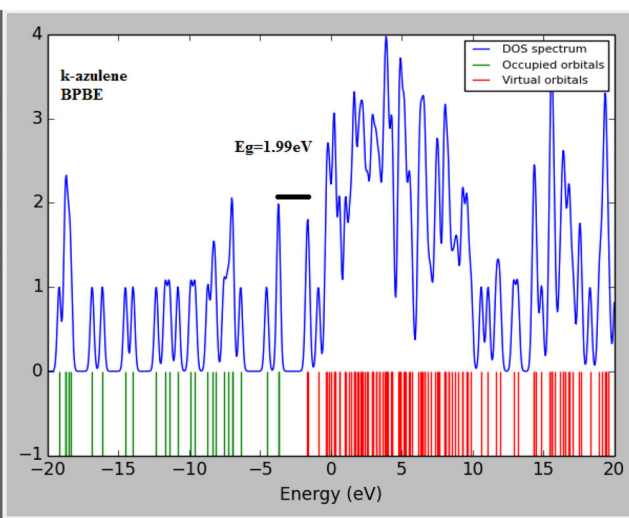
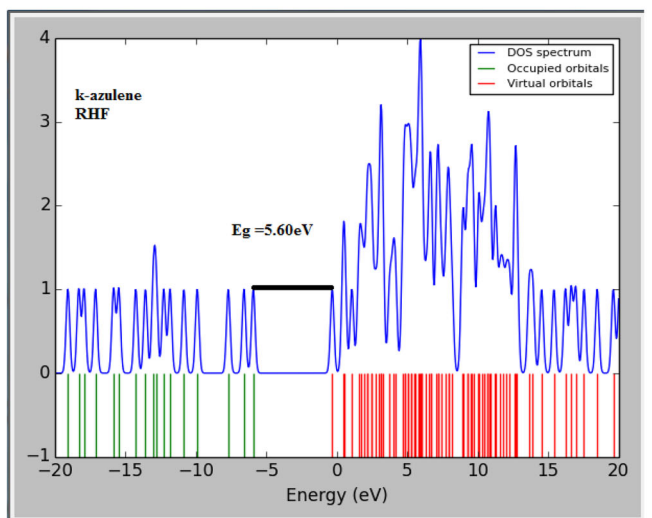
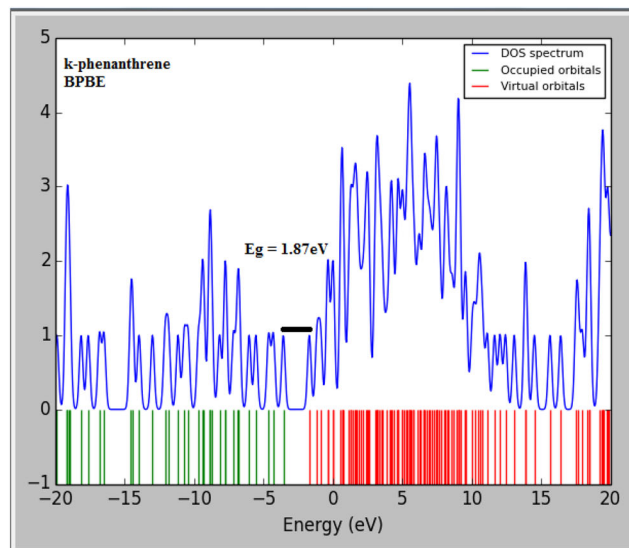
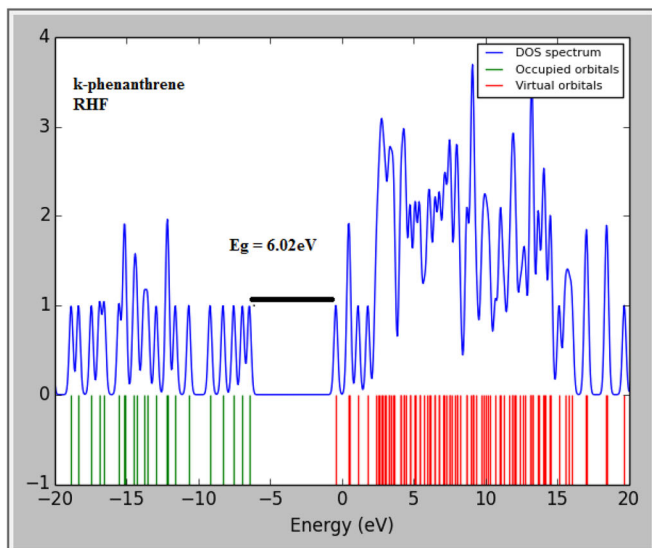


Fig. 4 Density of states (DOS) for k-phenanthrene, k-azulene and Rb-perylene, showing the largest band gap obtained at the hf and smallest band gap obtained at the bpbe methods

additionally smaller than that of the classical hole transfer material TPD (N, N'-diphenyl-N, N'-bis(3-methylphenyl)-(1,1'-biphenyl)-4,4'-diamine, with a hole reorganization energy $\lambda_h = 0.290$ eV [41, 72]

Consequently, these metalated GNRs have high short circuit current and are therefore characterized as emblematic transport material due to their high hole mobility. K-azulene has the smallest hole reorganization energy at any level of theory than any of the rest two molecules. We interest with the transport of holes, as we are characterizing donor materials which transfer holes after exciton dissociation. The carrier mobility of conjugated polymers are several orders of magnitude lesser than their crystalline counterparts due to recombinative carrier loss and could be improved by increasing carrier concentration and making sure that the conjugated polymer have a thin active layer that serve to reduce the optical absorption.

Fig. 5 Band gap against the hyperpolarizability for K-phenanthrene, K-azulene and Rb-perylene

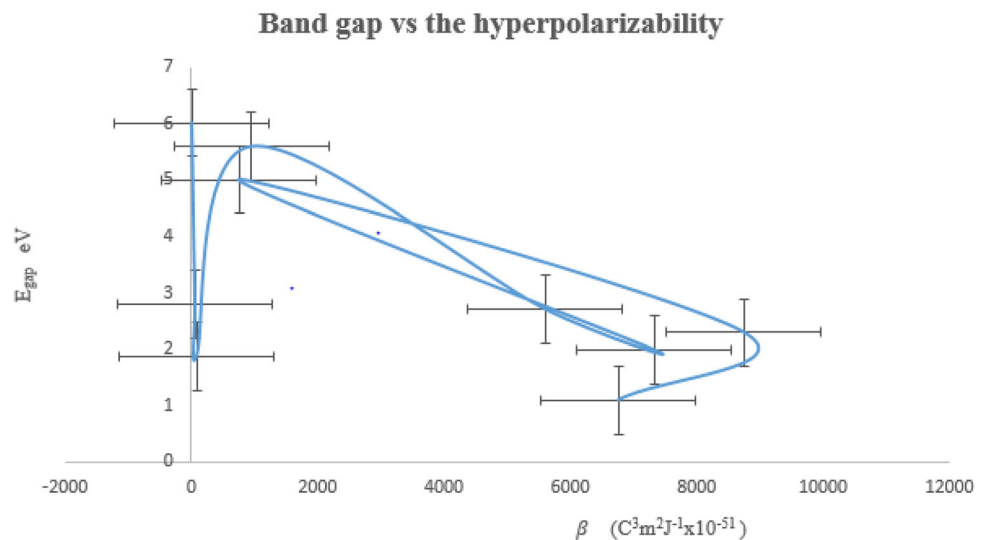


Table 2 Hole reorganization energy in eV for k-phenanthrene, k-azulene and Rb-perylene at the Rhf, B3lyp

	k-Phenanthrene			k-Azulene			Rb-perylene		
	Rhf	B3lyp	bpbe	Rhf	B3lyp	bpbe	Rhf	B3lyp	bpbe
λ_h /eV	0.183	0.218	0.251	0.168	0.159	0.167	0.240	0.261	0.256

3.2.3 Nonlinear optical behavior

Nonlinear optical (NLO) parameters such as α , $\Delta\alpha$, and β are of high relevance to comprehend the performance and behavior of OPVCs are shown in Table 3. These properties measures the extent of the delocalization of intramolecular charge for the donor electrons [73]. High values for NLO properties provide a higher efficiency of charge mobility from donor to acceptor. According to Balanay [74], this greatly affects short-circuit current density, as well as the solar cell system efficiency. In related literature, the increase in NLO properties in some organic dyes and porphyrins is directly related with the increment in the photovoltaic performance of those systems [74–76]. The NLO values of α , $\Delta\alpha$, and β are significantly amplified for the studied metalated GNRs and are equally pronounced as compared to values obtained in [50]. Comparing the hyperpolarizabilities of the metalated GNRs with the prototypic push-pull molecule, urea with hyperpolarizability $1.38 \times 10^{-51} \text{ C}^3 \text{ m}^2 / \text{J}^2$ [77–79], it is observed that all the studied metalated GNR have hyperpolarizabilities greater than the said urea except k-phenanthrene at the Rhf/6–31 + g(d,p). This indicates a significant charge mobility efficiency from the donor GNRs

Table 3 Nonlinear optical properties of k-phenanthrene, k-azulene and Rb-perylene at the Rhf, B3lyp and bpbe using the 6–31 + g(d,p) basis

	k-phenanthrene			k-azulene			Rb-perylene		
	Rhf	B3lyp	bpbe	Rhf	B3lyp	bpbe	Rhf	B3lyp	bpbe
$\alpha/c^2m^2/J \times 10^{-39}$	2.97	3.71	3.93	2.45	3.01	3.13	4.18	5.21	5.21
$\Delta\alpha/c^2m^2/J \times 10^{-40}$	16.4	24.2	26.9	3.27	24.26	1.84	3.21	2.22	9.33
$\beta/c^3m^2/J \times 10^{-52}$	8.32	58.45	80.66	950.98	5594.9	7318.72	752.29	8738.29	6756.0

metal derivative to acceptor PCBM. These high value of NLO properties are equally of interest in materials for emerging communication technologies and optical signals processing. The greatest NLO property is shown by Rb-perylene at all level theory.

Despite the incessant advances on the development of new organic polymers and innovative device engineering, the PCE of OPV devices has steadily improved to value of not more than 10% [21–24]. Nonetheless, this efficiency isn't adequate to meet the realistic specifications for commercialization, which emanates from the mismatch of the absorption of the photoactive material to the terrestrial solar spectrum.

4 Conclusion

Our computational results predicted, the photovoltaic properties of the some metalated GNRs to serve as donor material in OPV cells by using the rhf ab initio method, b3lyp and bpbe density functional methods along with the 6–31 + g(d,p). The materials possess a disapproving large band gap at the rhf and b3lyp/6–31 + g(d,p) level of theory as compared to the below 1.9 eV recommended value for OPVC, but with this value attained at the bpbe/6–31 + g(d,p)level of theory. Rb-perylene at the bpbe/6–31 + g(d,p)level of theory has the smallest band gap of 1.10 eV. They also have commendable small gap, when compared to traditional crystalline inorganic semiconductors materials, with well-placed position of HOMO and LUMO levels. The small hole reorganization energy when compared to the classical hole transport molecule TPD, shows that the donor semiconductor metal GNRs have a laudable hole mobility in the process of charge carrier

transmission and could therefore provide a high short circuit current. The best hole mobility is shown by K-azulene which also give the greatest value for the exciton dissociation linked parameter ΔE_{LL} . All the rest two molecules also have exciton dissociation value greater than the 0.3 eV minimum required value. The open circuit voltage falls moderately short of practical values especially at the dft methods, though hope to valorize it could stem from other determining factors like donor energy levels, chemical potential gradients, light intensity and morphology. The theoretical predicted value for PCE of our device for Rb-perylene may attain the 10% current mark for OPV cell which is a benchmark research finding and motivation for experimental consolidation of our theoretical work. This gives an additional incentive to design effective new photovoltaic materials efficient bulk heterojunction solar cells. The elevation of the efficiency realized in this research gets this organic polymer a step closer to commercialization. The NLO values of α , $\Delta\alpha$, and β are significantly amplified with β for the metalated GNRs greater than the prototypic push–pull molecule, urea. This would represent potential systems that would effectively transfer electronic charge from the donor to the acceptor.

Following the methodology established in the present work, there will be commendable future progress in the modelling of solar cell devices based upon OPV polymers based on GNRs metal derivatives. The approach of the present work may be an invaluable tool in acquiring accurate results in the development of innovative data sets of electronic structure properties on OPV polymer and for the fabrication of solar cells, getting these organic polymers a step closer to commercialization.

Acknowledgements

We are thankful to the Council of Scientific and Industrial Research (CSIR), India for financial support through Emeritus Professor scheme (Grant No. 21(0582)/03/EMR-II) to Late Prof. A.N. Singh of the Physics Department, Bahamas Hindu University, India which enabled him to purchase the Gaussian Software. We are most grateful to late Emeritus Prof. A.N. Singh for donating this software to one of us Prof. Geh Wilson Ejuh and to the Materials Science Laboratory of the University of Yaoundé I for enabling us use their computing facilities.

Compliance with ethical standards

Conflict of interest The authors declare that there is no conflict of interest as concern this article.

References

- V.W.W. Yam, *WOLEDs and Organic Photovoltaics* (Springer, Heidelberg, 2010)
- A. Marti Green, D. Ewan Dunlop, *Prog. Photovolt.* **27**(7), 565–575 (2019)
- J.F. Geisz, M.A. Steiner, N. Jain, *IEEE J. Photovolt.* **8**(2), 626–632 (2018)
- G.P. Smestad, F.C. Krebs, C.M. Lampert, C.G. Granqvist, *Sol. Energy Mater. Sol. Cells* **92**(4), 371–373 (2008)
- F. Padinger, R.S. Rittberger, N.S. Sariciftci, *Adv. Funct. Mater.* **13**, 85–88 (2003)
- C.J. Ko, Y.K. Lin, F.C. Chen, C.W. Chu, *Appl. Phys. Lett.* **90**(6), 063509 (2007)
- G. Li, V. Shrotriya, J. Huang, Y. Yao, T. Moriarty, K. Emery, *Nat. Mater.* **4**(11), 864–868 (2005)
- H. Yao, Y. Cui, D. Qian, S. Carlito, *J. Am. Chem. Soc.* **141**(19), 7743–7750 (2019)
- M. Reyes-Reyes, K. Kim, D.L. Carroll, *Appl. Phys. Lett.* **87**(8), 083506 (2005)
- Y. Li, J.D. Lin, X. Che, Y. Qu, F. Liu, L.S. Liao, *J. Am. Chem. Soc.* **139**(47), 17114–17119 (2017)
- B. O'Regan, M. Grätzel, *Nature* **353**, 737–740 (1991)
- K. Sayama, K. Hara, N. Mori, M. Satsuki, S. Suga, S. Tsukagoshi, Y. Abe, *Chem. Commun.* **13**, 1173–1174 (2000)
- C.J. Brabec, N.S. Sariciftci, J.C. Hummelen, *Adv. Funct. Mater.* **11**(1), 15–26 (2001)
- Y.J. Cheng, S.H. Yang, C.S. Hsu, *Chem. Rev.* **109**(11), 5868–5923 (2009)
- Y. Cui, H. Yao, J. Zhang, T. Zhang, Y. Wang, L. Hong, *Nat. Commun.* **10**, 2515 (2019)
- S. Günes, H. Neugebauer, N.S. Sariciftci, *Chem. Rev.* **107**(4), 1324–1338 (2007)
- R.S. Kularatne, H.D. Magurudeniya, P. Sista, M.C. Biewer, M.C. Stefan, *J. Polym. Sci. Part A* **51**, 743–768 (2013)
- S.B. Darling, F. You, *RSC Adv.* **3**, 17633 (2013)
- Y. Cui, H. Yao, L. Hong, T. Zhang, *Adv. Mat. Commun.* **31**(14), 1808356 (2019)
- N. Yeh, P. Yeh, *Renew. Sustain. Energy Rev.* **21**, 421–431 (2013)
- T. Yang, M. Wang, C. Duan, X. Hu, L. Huang, J. Peng, F. Huang, X. Gong, *Energy Environ. Sci.* **5**(8), 8208–8214 (2012)
- X. Li, W.C.H. Choy, L. Huo, F. Xie, W.E.I. Sha, B. Ding, X. Guo, Y. Li, J. Hou, J. You, *Adv. Mat.* **24**(22), 3046–3052 (2012)
- Z. He, C. Zhong, X. Huang, W.-Y. Wong, H. Wu, L. Chen, S. Su, Y. Cao, *Adv. Mat.* **23**(40), 4636–4643 (2011)
- Z. He, C. Zhong, S. Su, M. Xu, H. Wu, Y. Cao, *Nat. Photon* **6**, 591–595 (2012)
- H. Paul, C. David, B.P. Rand, *Acc. Chem. Res.* **42**(11), 1740–1747 (2009)
- M. Riede, T. Mueller, W. Tress, R. Schueppel, K. Leo, *Nanotechnology* **19**, 42 (2008)
- J. Roncali, *Macromol. Rapid Commun.* **28**(17), 1761–1775 (2007)
- N. Venkatram, M.A. Akundi, D. Narayana Rao, *Opt. Exp.* **13**, 867–872 (2005)
- F. Schedin, A.K. Geim, S.V. Morozov, E.W. Hill, P. Blake, M.I. Katsnelson, *Nat. Mater.* **6**, 652–655 (2007)
- M.D. Stoller, S. Park, Y. Zhu, J. An, R.S. Ruoff, *Nano Lett.* **8**, 3498 (2008)
- T.J. Echtermeyer, M.C. Lemme, M. Baus, B.N. Szafrank, A.K. Geim, H. Kurz, *IEEE Electron Device Lett.* **29**, 952 (2008)
- J.-S.K. Yu, C.-H. Yu, *J. Phys. Chem. A* **107**, 4268–4275 (2003)
- J.C. Hummelen, B.W. Knight, F. LePeq, F. Wudl, J. Yao, J. Org. Chem. **60**(3), 532–538 (1995)
- M.C. Scharber, D. Muhlbacher, M. Koppe, P. Denk, C. Waldauf, A.J. Heeger, C.J. Brabec, *Adv. Mat.* **18**(6), 789–794 (2006)
- A.D. Becke, *Phys. Rev. A* **38**, 3098 (1988)
- C. Lee, W. Yang, R.G. Parr, *Phys. Rev. B.* **37**, 785–789 (1988)
- J.P. Perdew, K. Burke, M. Ernzerhof, *Phys. Rev. Lett.* **77**, 3865 (1996)
- J.P. Perdew, K. Burke, M. Ernzerhof, *Phys. Rev. Lett.* **78**, 1396 (1997)
- M.J. Frisch, G.W. Trucks, H.B. Schlegel, G.E. Scuseria, M.A. Robb, J.R. Cheeseman, G. Scalmani, V. Barone, B.

- Mennucci, G.A. Petersson et al., *Gaussian 09, Revision B.01* (Gaussian Inc, Wallingford CT, 2009)
40. R. Dennington, T. Keith, J. Milam, *GaussView, Version 5* (Semichem Inc., Shawnee Mission KS, 2009)
41. N.K. Nkungli, J.N. Ghogomu, *J. Theor. Chem.* **1**, 11 (2016). <https://doi.org/10.1155/2016/7909576>
42. C. Herliette, A. Alongamo, N.K. Nkungli, J.N. Ghogomu, *J. Mol. Phys.* **117**(18), 2577–2592 (2019)
43. P. Ranjan, P. Verma, S. Agrawal, T.R. Rao, S.K. Samanta, A.D. Thakur, *Mat. Chem. Phys.* **226**, 350–355 (2019)
44. G.W. Ejuh, F. TchangnwaNya, N. Djongyang, J.M.B. Ndjaka, *SN Appl. Sci.* **2**, 1247 (2020)
45. G.W. Ejuh, F. Tchangnwa Nya, N. Djongyang, J.M.B. Ndjaka, *Opt. Quant. Electron.* **50**(9), 336 (2018)
46. A.H. Reshak, N.M. Abbass, J. Bila, M.R. Johan, I. Kityk, *J. Phys. Chem. C* **123**(44), 27172–27180 (2019)
47. M. Stolterfoht, P. Caprioglio, *Energy Environ. Sci.* **12**, 2778–2788 (2019)
48. S. Yang, J. Dai, Z. Yu, Y. Shao, Y. Zhou, *J. Am. Chem. Soc.* **141**(14), 5781–5787 (2019)
49. S.S. Shin, J.H. Suk, B.J. Kang, W. Yin, S.J. Lee, *Energy Environ. Sci.* **12**, 958–964 (2019)
50. A. Guillen-Lopez, M. Robles, J. Muniz, *Theor. Chem. Acc.* **137**(85), 1432–2234 (2018)
51. B.P. Rand, D.P. Burk, S.R. Forrest, *Phys. Rev. B* **75**(11), 115327 (2007)
52. Q.Q. Pan, S.B. Li, Y. Wu, G. Sun, Y. Geng, Z.M. Su, *RSC Adv.* **6**, 81164–81173 (2016)
53. D. Mhlbacher, M. Scharber, M. Morana, Z. Zhu, D. Waller, R. Gaudiana, C. Brabec, *Adv. Mat.* **18**(21), 2884–2889 (2006)
54. D. Wang, X. Zhang, W. Ding, X. Zhao, *Comput. Theory Chem.* **1029**, 68–78 (2014)
55. M. Sui, S. Li, Q. Pan, G. Sun, Y. Geng, *J. Mol. Model* **23**(28), 1610–2940 (2017)
56. Y.A. Duan, Y. Geng, H.B. Li, J.L. Jin, Y. Wu, Z.M. Su, *J. Comput. Chem.* **34**(19), 1611–1619 (2013)
57. J.D. Huang, W.L. Li, S.H. Wen, B. Dong, *J. Comput. Chem.* **36**(10), 695–706 (2015)
58. V. Lemaur, M. Steel, D. Beljonne, J.L. Brédas, *J. Am. Chem. Soc.* **127**(16), 6077–6086 (2005)
59. N.E. Gruhn, D.A. da Silva Filho, T.G. Bill, M. Malagoli, V. Coropceanu, A. Kahn, J.L. Brédas, *J. Am. Chem. Soc.* **124**(27), 7918–7919 (2002)
60. J.R. Reimers, *J. Chem. Phys.* **115**(20), 9103–9109 (2001)
61. V.T.T. Huong, H.T. Nguyen, M.T. Nguyen, *J. Phys. Chem. C* **117**(19), 10175–10184 (2013)
62. T. Mohr, V. Aroulmoji, R.S. Ravindran, M. Muller, S. Ranjitha, G. Rajarajan, P. Anbarasan, *Spectrochim. Acta Mol. Biomol Spectrosc.* **135**, 1066–1073 (2015)
63. A. Francisco, M.G. SantosaLuis, D. AbegãoofRuben, Fonseca. *J. Photochem. Photobiol. A* **369**, 70–76 (2019)
64. C. Yang, J. Zhang, N. Liang, H. Yao, *J. Mater. Chem. A* **32**(7), 18889–18897 (2019)
65. M. Horie, J. Kettle, C.Y. Yu, L.A. Majewski, S.W. Chang, J. Kirkpatrick, S.M. Tuladhar, *J. Mater. Chem.* **22**, 381–389 (2012)
66. K. Tvingstedt, K. Vandewal, A. Gadisa, F. Zhang, J. Manca, O. Inganäs, *J. Am. Chem. Soc.* **131**(33), 11819–11824 (2009)
67. D.B. Staple, P.A.K. Oliver, I.G. Hill, *Phys. Rev. B* **89**(20), 1719 (2014)
68. H. Alyar, *Rev. Adv. Mater. Sci.* **34**(1), 79–87 (2013)
69. R.A. Marcus, *Rev. Mod. Phys.* **65**(3), 599 (1993)
70. R.A. Marcus, *Annu. Rev. Phys. Chem.* **15**(1), 155–196 (1964)
71. M. Bourass, A. Touimi Benjelloun, M. Benzakour, M. Mcharfi, F. Jhilal, F. Serein-Spirau, *J. Saudi Chem. Soc.* **21**, 563–574 (2017)
72. R. Jin, K. Lia, X. Hana, *RSC Adv.* **9**, 22597–22603 (2019)
73. M. Senge, M. Fazekas, E. Notaras, W. Blau, M. Zawadzka, *Adv. Mater.* **19**(19), 2737–2774 (2007)
74. M.D. Balanay, O.H. Kim, *Curr. Appl. Phys.* **11**, 109–116 (2011)
75. C.R. Zhang, Z.J. Liu, Y.H. Chen, H.S. Chen, Y.Z. Wu, *Curr. Appl. Phys.* **10**(1), 77–83 (2010)
76. C.R. Zhang, Z.J. Liu, Y.H. Chen, H.S. Chen, Y.Z. Wu, *J. Mol. Struct. Theochem.* **899**, 86–93 (2010)
77. C.C. Fonkem, G.W. Ejuh, F. Tchangnwa Nyad, R.A. Yossa Kamsia, *Chin. J. Phys.* **63**, 207–212 (2020)
78. C. Karthika, S.R. SarathKumar, L. Kathuria, *Phys. Chem. Chem. Phys.* **21**, 11079–11086 (2019)
79. H. Tanak, A.A. Agar, O. Buyukgungor, *Spectrochim. Acta Part A* **118**(29), 672–682 (2014)

Publisher's Note Springer Nature remains neutral with regard to jurisdictional claims in published maps and institutional affiliations.